



1 Light-induced protein nitration and degradation with HONO 2 emission

3 Hannah Meusel¹, Yasin Elshorbany², Uwe Kuhn¹, Thorsten Bartels-Rausch³, Kathrin Reinmuth-
4 Selzle¹, Christopher J. Kampf⁴, Guo Li¹, Xiaoxiang Wang¹, Jos Lelieveld⁵, Ulrich Pöschl¹,
5 Thorsten Hoffmann⁶, Hang Su^{1,7*}, Markus Ammann³, Yafang Cheng^{1,7*}

6 ¹ Max Planck Institute for Chemistry, Multiphase Chemistry Department, Mainz, Germany

7 ² NASA Goddard Space Flight Center, Greenbelt, Maryland, USA & Earth System Science Interdisciplinary Center,
8 University of Maryland, College Park, Maryland, USA

9 ³ Paul Scherer Institute, Villigen, Switzerland

10 ⁴ Johannes Gutenberg University, Institute for Organic Chemistry, Mainz, Germany

11 ⁵ Max Planck Institute for Chemistry, Atmospheric Chemistry Department, Mainz, Germany

12 ⁶ Johannes Gutenberg University, Institute for Inorganic and Analytical Chemistry, Mainz, Germany

13 ⁷ Institute for Environmental and Climate Research, Jinan University, Guangzhou, China

14 * Correspondence to: Y. Cheng (yafang.cheng@mpic.de) or H. Su (h.su@mpic.de)

15 **Abstract.** Proteins can be nitrated by air pollutants (NO₂), enhancing their allergenic potential. This work provides
16 insight into protein nitration and subsequent decomposition in the presence of solar radiation. We also investigated
17 light-induced formation of nitrous acid (HONO) from protein surfaces that were nitrated either online with
18 instantaneous gas phase exposure to NO₂ or offline by an efficient nitration agent (tetranitromethane, TNM). Bovine
19 serum albumin (BSA) and ovalbumin (OVA) were used as model substances for proteins. Nitration degrees of about
20 1% were derived applying NO₂ concentrations of 100 ppb under VIS/UV illuminated condition, while simultaneous
21 decomposition of (nitrated) proteins was also found during long-term (20h) irradiation exposure. Gas exchange
22 measurements of TNM-nitrated proteins revealed that HONO can be formed and released even without contribution
23 of instantaneous heterogeneous NO₂ conversion. However, fumigation with NO₂ was found to increase HONO
24 emissions substantially. In particular, a strong dependence of HONO emissions on light intensity, relative humidity
25 (RH), NO₂ concentrations and the applied coating thickness were found. The 20 hours long-term studies revealed
26 sustained HONO formation, even if concentrations of the intact (nitrated) proteins were too low to be detected after
27 the gas exchange measurements. A reaction mechanism for the NO₂ conversion based on the Langmuir-Hinshelwood
28 kinetics is proposed.

29 1 Introduction

30 Primary biological aerosols (PBA), or bioaerosols, including proteins, from different sources and with distinct
31 properties, are known to influence atmospheric cloud microphysics and public health (Lang-Yona et al., 2016;
32 D'Amato et al., 2007; Pummer et al., 2015). Bioaerosols represent a diverse subset of atmospheric particulate matter
33 that is directly emitted in form of active or dead organisms, or fragments, like bacteria, fungal spores, pollens,
34 viruses, and plant debris. Proteins are found ubiquitously in the atmosphere as part of these airborne, typically
35 coarse-size biological particles (diameter > 2.5 μm), but also in fine particulate matter (diameter < 2.5 μm)
36 associated with a host of different constituents such as polymers derived from biomaterials and proteins dissolved in

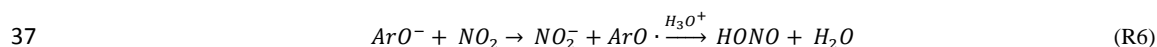
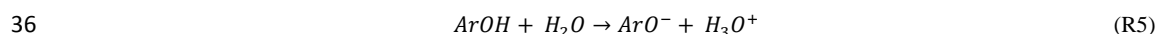
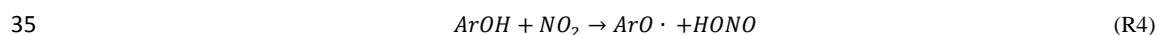
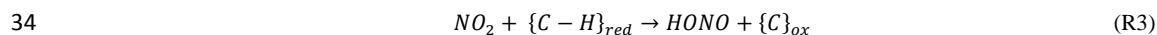
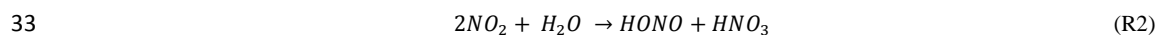


1 hydrometeors, mixed with fine dust and other particles (Miguel et al. 1999; Riediker et al., 2000; Zhang and
 2 Anastasio, 2003). Proteins contribute up to 5% of particle mass in airborne particles (Franze et al., 2003a; Staton et
 3 al., 2015; Menetrez et al., 2007) and are also found at surfaces of soils and plants. Proteins can be nitrated and are
 4 then likely to enhance allergic responses (Gruijthuijsen et al., 2006). Nitrogen dioxide ($\bullet\text{NO}_2$) has emerged as an
 5 important biological reactant and has been shown to be capable of electron (or H atom) abstraction from the amino
 6 acid tyrosine (Tyr) to form TyrO \bullet in aqueous solutions (tyrosine phenoxyl radical, also called tyrosyl radical; Prütz et
 7 al. 1984 and 1985; Alfassi 1987; Houée-Lévin et al., 2015), which subsequently can be nitrated by a second NO_2
 8 molecule. Shiraiwa et al. (2012) observed nitration of protein aerosol, but not solely with NO_2 in the gasphase, and
 9 demonstrated that simultaneous O_3 exposure of airborne proteins in dark conditions can significantly enhance NO_2
 10 uptake and consequent protein nitration (3-nitrotyrosine formation) by way of direct O_3 -mediated formation of the
 11 TyrO \bullet intermediate. A connection between increased allergic diseases and elevated environmental pollution,
 12 especially traffic-related air pollution has been proposed (Ring et al., 2001). Tyrosine is one of the photosensitive
 13 amino acids and it is subject of direct and indirect photo-degradation under solar-simulated conditions (Boreen, et al.,
 14 2008), especially mediated by both UV-B (λ 280–320 nm) and UV-A (λ 320–400 nm) radiation (Houee-Levin et al.,
 15 2015; Bensasson et al., 1993). Direct light absorption or absorption by adjacent endogenous or exogenous
 16 chromophores and subsequent energy transfer results in an electronically-excited state of tyrosine (for details see
 17 Houée-Lévin et al. 2015 and references therein). If the triplet state of tyrosine is generated, it can undergo electron
 18 transfer reactions and deprotonation to yield TyrO \bullet (Fig.1, Bensasson 1993; Davies 1991; Berto et al., 2016).
 19 Regardless of how the tyrosyl radical is generated, it can be nitrated by reaction with NO_2 , but also hydroxylated or
 20 dimerized (Shiraiwa et al., 2012; Reinmuth-Selzle et al., 2014; Kampf et al., 2015).

21 With respect to atmospheric chemistry, Bejan et al. (2006) have shown that photolysis of ortho-nitrophenols (as is
 22 the case for 3-nitrotyrosine) can generate nitrous acid (HONO). HONO is of great interest for atmospheric
 23 composition, as its photolysis forms OH radicals, being the key oxidant for degradation of most air pollutants in the
 24 troposphere (Levy, 1971). In the lower atmosphere, up to 30% of the primary OH radical production can be
 25 attributed to photolysis of HONO, especially during the early morning when other photochemical OH sources are
 26 still small (R1, Kleffmann et al., 2005; Aliche et al., 2002; Ren et al., 2006; Su et al., 2008; Meusel et al. 2016).



28 HONO can be directly emitted by combustion of fossil fuel (Kurtenbach et al., 2001) or formed by gas phase
 29 reactions of NO and OH (the backwards reaction of R1) and heterogeneous reactions of NO_2 on wet surfaces
 30 according to R2. On carbonaceous surfaces (soot, phenolic compounds) HONO is formed via electron or H transfer
 31 reactions (R3 and R4-R6; Kalberer et al., 1999; Kleffmann et al., 1999; Gutzwiller et al., 2002; Aubin and Abbatt
 32 2007; Han et al., 2013; Arens et al., 2001, 2002; Ammann et al., 1998, 2005).





1 Previous atmospheric measurements and modeling studies have shown unexpected high HONO concentrations
2 during daytime, which can also contribute to aerosol formation through enhanced oxidation of precursor gases
3 (Elshorbany et al., 2014). Measured mixing ratios are typically about one order of magnitude higher than simulated
4 ones, and an additional source of 200-800 ppt h⁻¹ would be required to explain observed mixing ratios (Kleffmann et
5 al., 2005; Acker et al., 2006; Sörgel et al., 2011; Li et al., 2012; Su et al., 2008; Elshorbany et al., 2012; Meusel et al.,
6 2016) indicating that estimates of daytime HONO sources are still under debate. It was suggested that HONO arises
7 from the photolysis of nitric acid and nitrate or by heterogeneous photochemistry of NO₂ on organic substrates and
8 soot (Zhou et al., 2001; 2002 and 2003; Villena et al., 2011; Ramazan et al., 2004; George et al., 2005; Sosedova et
9 al., 2011; Monge et al., 2010; Han et al., 2016). Stemmler et al. (2006, 2007) found HONO formation on light-
10 activated humic acid, and field studies showed that HONO formation correlates with aerosol surface area, NO₂ and
11 solar radiation (Su et al., 2008; Reisinger, 2000; Costabile et al., 2010; Wong et al., 2012; Sörgel et al., 2015) and is
12 increased during foggy periods (Notholt et al., 1992). Another proposed source of HONO is the soil, where it has
13 been found to be co-emitted with NO by soil biological activities (Oswald et al., 2013; Su et al., 2011; Weber et al.,
14 2015).

15 In view of light-induced nitration of proteins and HONO formation by photolysis of nitro-phenols, light-enhanced
16 production of HONO on protein surfaces can be anticipated, which, to the best of our knowledge, has not been
17 studied before.

18 This work aims at providing insight into protein nitration, the atmospheric stability of the nitrated protein, and
19 respective formation of HONO from protein surfaces that were nitrated either offline in liquid phase prior to the gas
20 exchange measurements, or online with instantaneous gas phase exposure to NO₂, with particular emphasis on
21 environmental parameters like light intensity, relative humidity (RH) und NO₂ concentrations. Bovine serum
22 albumin (BSA), a globular protein with a molecular mass of 66.5 kDa and 21 tyrosine residues per molecule, was
23 chosen as a well-defined model substance for proteins. Nitrated ovalbumin (OVA) was used to study the light-
24 induced degradation of proteins that were nitrated prior to gas exchange measurements. This well-studied protein has
25 a molecular mass of 45 kDa and 10 tyrosine residues per molecule.

26 **2 Materials and methods**

27 **2.1 Protein preparation and analysis**

28 BSA (albumin from bovine serum, Cohn V fraction, lyophilized powder, ≥ 96%; Sigma Aldrich, St. Louis, Missouri,
29 USA) or nitrated OVA (ovalbumin) was solved in pure water (18.2MΩ cm) and coated onto the glass tube.

30 The nitration of ovalbumin (OVA) was described previously (Yang et al., 2010; Zhang et al., 2011). Briefly, OVA
31 (Grade V, A5503-5G, Sigma Aldrich, Germany) was dissolved in phosphate buffered saline PBS (P4417-50TAB,
32 Sigma Aldrich, Germany) to a concentration of 10 mg/ml. 50 μl tetranitromethane TNM (T25003-5G, Sigma
33 Aldrich, Germany) dissolved in methanol 4% (v/v) were added to a 2.5 ml aliquot of the OVA solution and stirred
34 for 180 min at room temperature. Size exclusion chromatography columns (PD-10 Sephadex G-25 M, 17-0851-01,
35 GE Healthcare, Germany) were used for clean-up. The eluate was dried in a freeze dryer and stored in a refrigerator
36 at 4°C.



1 After the flow-tube-experiments (see below) the proteins were extracted with water from the tube and analyzed with
2 liquid chromatography (HPLC-DAD; Agilent Technologies 1200 series) according to Selzle et al. (2013). This
3 method provides a straightforward and efficient way to determine the nitration of proteins. Briefly, a monomerically
4 bound C18 column (Vydac 238TP, 250 mm×2.1 mm inner diameter, 5 μm particle size; Grace Vydac, Alltech) was
5 used for chromatographic separation. Eluents were 0.1 % (v/v) trifluoroacetic acid in water (LiChrosolv) (eluent A)
6 and acetonitrile (ROTISOLV HPLC Gradient Grade, Carl Roth GmbH + Co. KG, Germany) (eluent B). Gradient
7 elution was performed at a flow rate of 200 μL/min. ChemStation software (Rev. B.03.01, Agilent) was used for
8 system control and data analysis. For each chromatographic run, the solvent gradient started at 3% B followed by a
9 linear gradient to 90% B within 15 min, flushing back to 3% B within 0.2 min, and maintaining 3% B for additional
10 2.8 min. Column re-equilibration time was 5 min before the next run. Absorbance was monitored at wavelengths of
11 280 and 357 nm. The sample injection volume was 10-30 μL. Each chromatographic run was repeated three times.
12 The protein nitration degree was determined by the method of Selzle et al. (2013). Native and un-treated BSA did not
13 show any degree of nitration.

14 2.2 Coated-wall flow tube system

15 Figure 2 shows a flowchart of the set-up of the experiment. NO₂ was provided in a gas bottle (1 ppm in N₂, Carbagas
16 AG, Grümligen, Switzerland). NO₂ was further diluted (mass flow controller, MFC3) with humidified pure nitrogen
17 to achieve NO₂ mixing ratios between 20 and 100 ppb. Impurities of HONO in the NO₂-gas cylinder were removed
18 by means of a HONO scrubber. The Na₂CO₃ trap was prepared by soaking 4mm firebrick in a saturated Na₂CO₃ in
19 50% ethanol / water solution and drying for 24 hours. The impregnated firebrick granules were put into a 0.8 cm
20 inner diameter and 15 cm long glass tube, which was closed by quartz wool plugs on both sides. A constant total
21 flow was provided by means of another N₂ mass flow controller (MFC2) that compensated for changes in NO₂
22 addition. Different fractions of total surface areas (50, 70 and 100%) of the reaction tube (50 cm x 0.81 cm i.d.) were
23 coated with 2 mg BSA or nitrated OVA, respectively. Therefore 2 mg protein was dissolved in 600 μL pure water,
24 injected into the tube and then gently dried in a low humidity N₂ flow (RH ~ 30-40%) with continuous rotation of the
25 tube. The coated reaction tube was exposed to the generated gas mixture and irradiated with either (i) 1, 3 or 7 VIS
26 lights (400-700 nm; L 15 W/954, lumilux de luxe daylight, Osram, Augsburg, Germany) which is 0, 23, 69 or 161 W
27 m⁻² respectively or (ii) 4 VIS and 3 UV lights (340-400 nm; UV-A, TL-D 15 W/10, Philips, Hamburg, Germany).

28 An overview of the experiments performed during this study is shown in table 1. Light induced decomposition of
29 nitrated proteins was studied on OVA. Instantaneous NO₂ transformation and its light- and RH- dependence on
30 heterogeneous HONO formation were studied on BSA in short-term experiments. Extended studies on BSA were
31 performed to explore the persistence of the surface reactivity and respective catalytic effects.

32 A commercial long path absorption photometry instrument (LOPAP, QUMA) was used for HONO analysis. The
33 measurement technique was introduced by Heland et al. (2001). This wet chemical analytical method has an
34 unmatched low detection limit of 3-5 ppt with high HONO collection efficiency (≥ 99%). HONO is continuously
35 trapped in a stripping coil flushed with an acidic solution of sulfanilamide. In a second reaction with n-(1-
36 naphthyl)ethylenediamine-dihydrochloride an azo dye is formed, whose concentration is determined by absorption
37 photometry in a long Teflon tubing. LOPAP has two stripping coils in series to reduce known interferences. In the



1 first stripping coil HONO is quantitatively collected. Due to the acidic stripping solution, interfering species are
2 collected less efficiently but in both channels. The true concentration of HONO is obtained by subtracting the
3 interferences quantified in the second channel from the total signal obtained in the first channel. The accuracy of the
4 HONO measurements was 10%, based on the uncertainties of liquid and gas flow, concentration of calibration
5 standard and regression of calibration.

6 The reagents were all high-purity-grade chemicals, i.e., hydrochloric acid (37 %, ACS reagent, Sigma Aldrich, St.
7 Louis, Missouri, USA), sulfanilamide (for analysis, >99 %; Sigma Aldrich) and N-(1-naphthyl)-ethylenediamine
8 dihydrochloride (>98%; ACS reagent, Fluka by Sigma Aldrich). For calibration Titrisol® 1000 mg NO₂⁻ (NaNO₂ in
9 H₂O; Merck) was diluted to 0.001 mg/L NO₂⁻. For preparation of all solutions and for cleaning of the absorption
10 tubes 18MΩ H₂O was used.

11 NO_x concentrations were analyzed by means of a commercial chemiluminescence detector from EcoPhysics (CLD
12 77 AM, Duernten, Switzerland).

13 **3 Results and discussion**

14 **3.1 BSA nitration and degradation**

15 Nitrate proteins can lead to a stronger allergic response. Nitration of proteins can be enhanced by O₃ activation (in
16 the dark). In the environment, about half a day light is present. What happens with irradiated proteins when exposed
17 to NO₂. Can they be nitrated efficiently? To investigate the degree of protein nitration under illuminated conditions,
18 BSA coated on the reaction tube (17.5 μg cm⁻²) was exposed to 7 VIS lamps (40% of a clear sky irradiance for a
19 solar zenith of 48°; Stemmler et al., 2006) and 100 ppb NO₂ at 70% RH. After 20 hours the BSA nitration degree
20 (ND, concentration of nitrated tyrosine residues divided by the total concentration of tyrosine residues) investigated
21 by means of the HPLC-DAD method was (1.0 ± 0.1)%. Introducing UV radiation (4 VIS plus 3 UV lamps) resulted
22 in a slightly higher ND of (1.1 ± 0.1)%. Note that no intact protein could be detected by HPLC-DAD after another 20
23 hours of irradiation without NO₂, indicating light induced decomposition of proteins. However, the applied HPLC-
24 DAD technique only detects (nitro-)tyrosine residues in proteins, and does not provide information about protein
25 fragments or single nitrated or non-nitrated tyrosine residues. Hence, proteins might have been decomposed while
26 tyrosine remains in its nitrated form, not detectable by our analysis method. Similarly, proteins (here: OVA) that
27 were nitrated with TNM in aqueous phase prior to coating (21.5 μg cm⁻²) to an extent of 12.5% also decomposed
28 when illuminated about 6 hours (1-7 VIS lights; with and without 20 ppb NO₂). Thus the nitration of proteins by
29 light and NO₂ was confirmed, but with simultaneous gradual decomposition of the proteins. Effects of UV irradiation
30 (240-340 nm) on proteins containing aromatic amino acids were reviewed previously (Neves-Peterson et al., 2012).
31 It was shown that triplet state tryptophan and tyrosine can transfer electron to a nearby disulfide bridge to form the
32 tryptophan and tyrosine radical. The disulfide bridge could break leading to conformational changes in the protein
33 but not necessarily resulting in inactivation of the protein. In strong UV light (≈200 nm) the peptide bond could also
34 break (Nikogosyan and Görner, 1999).

35 Franze et al. (2005) analyzed a variety of natural samples (road dust, window dust and particulate matter PM 2.5)
36 collected in the metropolitan area of Munich, containing 0.08-21 g/kg proteins, and revealed equivalent degrees of



1 nitration (EDN, concentration of nitrated protein divided by concentration of all proteins) between 0.01 and 0.1%
2 only. Such low nitration degree is in line with light induced decomposition of (nitrated) proteins. On the other hand,
3 an EDN up to 10% (average 5%) was found for BSA and birch pollen extract (BPE) exposed to Munich ambient air
4 for two weeks under dark conditions, with daily mean NO₂ (O₃) concentration of 17 to 50 ppb (7 to 43 ppb) in the
5 same study, suggesting the deficiency of decomposition without being irradiated. BSA and OVA loaded on syringe-
6 filters and exposed to 200 ppb NO₂/O₃ for 6 days under dark conditions were nitrated to 6 and 8%, respectively
7 (Yang et al., 2010). Reinmuth-Selzle et al. (2014) found similar ND for major birch pollen allergen Bet v 1 loaded on
8 syringe-filters exposed to 80-470 ppb NO₂ and O₃. When exposed for 3-72 hours to NO₂/O₃ at RH < 92% the ND
9 was 2-4%, while at condensing conditions (RH > 98%) the ND increased to 6% after less than one day (19 hours).
10 The ND of Bet v 1 was considerably increased to 22% for proteins solved in the aqueous phase (0.16 mg mL⁻¹) when
11 bubbling with a 120 ppb NO₂/O₃ gas mixture for a similar period of time (17 hours). Other nitration methods,
12 investigated by Reinmuth-Selzle et al. (2014), e.g., nitration of Bet v 1 with peroxyxynitrite (ONOO[•], formed by
13 reaction of NO with O₂[•]) or TNM lead to ND between 10 and 72% depending on reaction time, reagent concentration
14 and temperature. Similarly high NDs of 45-50% were obtained by aqueous phase TNM nitration of BSA and OVA
15 by Yang et al. (2010).

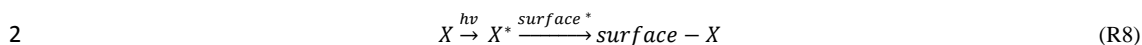
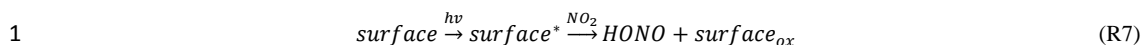
16 3.2 HONO formation

17 3.2.1 HONO formation from nitrated proteins

18 Strong HONO emissions were found for OVA nitrated in the liquid phase prior to gas exchange measurements (ND
19 = 12.5%). A strong correlation between HONO emission and light intensity was observed (50% RH; Fig. 3). Initially,
20 we did not apply NO₂. Thus the observed HONO formation (up to 950 ppt) originated from decomposing nitrated
21 proteins rather than from heterogeneous conversion of NO₂. However, when exposed to 20 ppb of NO₂ in dark
22 conditions, HONO formation increased 4-fold (50 to 200 ppt), and about 2-fold with 7 VIS lamps turned on (950 to
23 1800 ppt). After 7 hours of flow tube experiments (4.5 h irradiation with varying light intensities (0-1-3-7 lights) +
24 2.5 h irradiation/20 ppb NO₂ (7-3-0- lights)), no intact protein was found according to the analysis of HPLC-DAD.

25 3.2.2 Light dependency

26 To investigate HONO formation on unmodified BSA coating (31.4 μg cm⁻²) in dependence on light conditions, the
27 radiation intensity (number of VIS lamps) was changed under otherwise constant conditions of exposure at 20 ppb
28 NO₂ and 50% RH. Decreasing light intensity revealed a linearly decreasing trend in HONO formation from about
29 1000 ppt to 140 ppt (red symbols in Fig. 4). After re-illumination to the initial high light intensity the HONO
30 formation was reduced by 32% (blue symbol in Fig. 4). Stemmler et al. (2006) and Sosedova et al. (2011) also
31 observed a similar saturation of HONO formation on humic acid, tannic and gentisic acid at higher light intensities.
32 Stemmler et al. (2006) argued that surface sites activated for NO₂ heterogeneous conversion by light (R3) would
33 become de-activated by competition with photo-induced oxidants (X^{*}, R7-8), e.g., primary chromophores or electron
34 donors are oxidized by surface*, which is in line with the observed decomposition of the native protein presented
35 above.



3 In other studies the NO₂ uptake coefficient on soot, mineral dust, humic acid and other solid organic compounds
 4 similarly increased at increasing light intensities (George et al., 2005; Stemmler et al., 2007; Ndour et al., 2008;
 5 Monge et al., 2010; Han et al., 2016). Note that the HONO yield (ratio of HONO formed to NO₂ lost) was found to
 6 be constant at light intensities in the range of 60-200 W m⁻² in the work of Han et al. (2016), but have shown a linear
 7 dependence on light for nitrated phenols (Bejan et al., 2006).

8 3.2.3 NO₂ dependency

9 At about 50% relative humidity and high illumination intensities (7 VIS lamps, ~161 W m⁻²), heterogeneous
 10 formation of HONO strongly correlated with the applied NO₂ concentration (Fig. 5). On a BSA surface of about 16.1
 11 μg cm⁻² (Tab. 1) the produced HONO concentration increased from 56 ppt at 20 ppb NO₂ to 160 ppt at 100 ppb NO₂.
 12 Only at a threshold NO₂ level well above those typically observed in natural environments (>>150 ppb) this
 13 increasing trend slowed down to some extent, indicative of saturation of active surface sites. A similar pattern of
 14 NO₂ dependence was also observed for light-induced HONO formation from humic acid (Stemmler et al., 2006) and
 15 phenolic compounds like gentisic and tannic acid (Sosedova et al., 2011), and for heterogeneous NO₂ conversion on
 16 soot under dark conditions (Stadler and Rossi, 2000; Salgado and Rossi, 2002; Arens et al., 2001).

17 For better comparison of the different studies the HONO concentration measured at different NO₂ concentrations
 18 was normalized to the HONO concentration at 20 ppb NO₂ ([HONO]_{NO2}/[HONO]_{NO2=20ppb}) in Fig. 5, as variable
 19 absolute amounts of HONO were found in different studies and matrices. A cease of the NO₂ dependency on
 20 heterogeneous HONO formation can be assessed for most of the studies at NO₂ concentrations ≥ 200 ppb. A very
 21 similar correlation (up to 40 ppb NO₂) was observed when NO₂ was applied additionally during the gas phase
 22 photolysis of nitrophenols (fig. 5; Bejan et al., 2006). Even though the matrix (nitrophenols) and conditions
 23 (illuminated) of the latter is comparable to the experiment presented here, for BSA no clear indication of saturation
 24 was found up to 160 ppb of NO₂, pointing to a highly reactive surface of BSA for NO₂ under illuminated conditions.
 25 As shown with R7 and R8, the concentration dependence depends on the competing channel R8, therefore, this is
 26 strongly matrix dependent, both in terms of chemical and physical properties.

27 3.2.4 Impact of coating thickness

28 Strong differences in HONO concentrations were found for experiments with different coating thicknesses applying
 29 otherwise similar conditions (20 ppb of NO₂, 7 VIS lamps and 50% RH). While only 55 ppt of HONO concentration
 30 was observed for a shallow homogeneous coating of 16.1 μg cm⁻² (217.6 nm thickness, see below) applied on the
 31 whole length of the tube, up to 2 ppb were found for a thick (more uneven) coating of 31.44 μg cm⁻² (435.2 nm
 32 thickness) covering only 50% of the tube (Fig. 6). Potential explanations are that thicker coating leads to (1) more
 33 bulk reactions producing HONO, or (2) different morphologies, e.g., higher effective reaction surfaces.

34 A strong increase in NO₂ uptake coefficients with increasing coating thickness was also observed for humic acid
 35 coatings (Han et al., 2016). However, they found an upper threshold value of 2 μg cm⁻² of cover load (20 nm



1 absolute thickness, assuming a humic acid density of 1 g cm^{-3} , above which uptake coefficients were found to be
2 constant. The authors also proposed that NO_2 can diffuse deeper into the coating and below $2 \mu\text{g cm}^{-2}$ the full cover
3 depth would react with NO_2 , respectively.

4 For proteins the number of molecules per monolayer depends on their orientation and respective layer thickness can
5 vary accordingly. One (dry, crystalline) BSA molecule has a volume of about 154 nm^3 (Bujacz, 2012). In a flat
6 orientation (4.4 nm layer height, and a projecting area of 35 nm^2 per molecule) 3.64×10^{14} molecules ($40.5 \mu\text{g}$; 0.32
7 $\mu\text{g cm}^{-2}$) of BSA are needed to form one complete monolayer in the flow tube (i.d. of 0.81 cm, 50 cm length, 100%
8 surface coating). Hence, the thinnest BSA coating applied in the experiment ($16.1 \mu\text{g cm}^{-2}$) would consist of 50
9 monolayers revealing a total coating thickness of 217.6 nm, and the thickest BSA coating ($31 \mu\text{g cm}^{-2}$) would have
10 99 monolayers and an absolute thickness of 435.1 nm. At the other extreme (non-flat) orientation, more BSA
11 molecules are needed to sustain one monolayer. With 21.7 nm^2 of projected area of one molecule and 7.1 nm
12 monolayer height, 5.86×10^{14} molecules of BSA are needed to form one complete monolayer in the flow tube. The
13 coatings would consist of between 31 (thinnest) and 61 (thickest) monolayers of BSA. With a flat orientation 1-2%
14 (number or weight) of BSA molecules would build the uppermost surface monolayer, whereas in an upright
15 molecule orientation 1.6-3.3% would be in direct contact with surface ambient air.

16 In the crystalline form several molecules of water stick tightly to BSA. As BSA is highly hygroscopic, more water
17 molecules are adsorbed at higher relative humidity. At 35% RH BSA is deliquesced (Mikhailov et al., 2004).
18 Therefore the above described number of monolayers and the absolute layer thickness are a lower bound estimate.

19 Conclusively, the thickness dependence on HONO formation is extremely complex. Activation and photolysis of
20 nitrated Tyr occurs throughout the BSA layer. The heterogeneous reaction of NO_2 may or may be not limited to the
21 surface depending on solubility and diffusivity of NO_2 . Also the release of HONO may be limited by diffusion.

22 3.2.5 RH dependency

23 The dependence of HONO emission on relative humidity is shown in Fig. 7. Here about 25 ppb of NO_2 was applied
24 to a (not nitrated) BSA coated flow tube ($17.5 \mu\text{g cm}^{-2}$) both in dark and illuminated conditions (7 VIS lights).
25 HONO formation scaled with relative humidity. Kleffmann et al. (1999) proposed that higher humidity inhibits the
26 self-reaction of HONO ($2 \text{ HONO}_{(s,g)} \rightarrow \text{NO}_2 + \text{NO} + \text{H}_2\text{O}$), which leads to higher HONO yield from heterogeneous
27 NO_2 conversion.

28 The RH dependence of HONO formation on proteins is different to other surfaces. For example, no influence of RH
29 has been observed for dark heterogeneous HONO formation on soot particles sampled on filters (Arens et al., 2001).
30 For HONO formation on tannic acid coatings (both at dark and irradiated conditions) a linear but relatively weak
31 dependence has been reported between 10 and 60% RH, while below 10% and above 60% RH the correlation
32 between HONO formation and RH was much stronger (Sosedova et al., 2011). Similar results were observed for
33 anthrarobin coatings by Arens et al. (2002). This type of dependence of HONO formation on phenolic surfaces on
34 RH equals the HONO formation on glass, following the BET water uptake isotherm of water on polar surfaces
35 (Finnlayson-Pitts et al., 2003; Summer et al., 2004). For humic acid surfaces the NO_2 uptake coefficients also weakly
36 increased below 20% RH and were found to be constant between 20 and 60% (Stemmler et al., 2007).



1 While on solid matter chemical reactions are essentially confined to the surface rather than in the bulk, proteins can
2 adopt an amorphous solid or semisolid state, influencing the rate of heterogeneous reactions and multiphase
3 processes. Molecular diffusion in the non-solid phase affects the gas uptake and respective chemical transformation.
4 Shiraiwa et al. (2011) could show that the ozonolysis of amorphous protein is kinetically limited by bulk diffusion.
5 The reactive gas uptake exhibits a pronounced increase with relative humidity, which can be explained by a decrease
6 of viscosity and increase of diffusivity, as the uptake of water transforms the amorphous organic matrix from a
7 glassy to a semisolid state (moisture-induced phase transition). The viscosity and diffusivity of proteins depend
8 strongly on the ambient relative humidity because water can act as a plasticizer and increase the mobility of the
9 protein matrix (for details see Shiraiwa et al. 2011 and references therein). Shiraiwa et al. (2011) further showed that
10 the BSA phase changes from solid through semisolid to viscous liquid as RH increases, while trace gas diffusion
11 coefficients increased about 10 orders of magnitude. This way, characteristic times for heterogeneous reaction rates
12 can decrease from seconds to days as the rate of diffusion in semisolid phases can decrease by multiple orders of
13 magnitude in response to both low temperature (not investigated in here) and/or low relative humidity. Accordingly,
14 we propose that HONO formation rate depends on the condensed phase diffusion coefficients of NO₂ diffusing into
15 the protein bulk, HONO released from the bulk and mobility of excited intermediates.

16 3.2.6 Long term exposure with NO₂ under irradiated conditions

17 To study long-term effects of irradiation on HONO formation from proteins, flow tubes were coated with 2 mg BSA
18 ($17.5 \pm 0.4 \mu\text{g cm}^{-2}$; 90% of total length) and exposed to 100 ppb NO₂, at 80% RH at illuminated conditions for a
19 time period of up to 20 hours (Fig. 8). Samples illuminated with VIS light only (red and orange colored lines in Fig.
20 8) showed persistent HONO emissions over the whole measurement period. For reasons unknown, and even though
21 the observed HONO concentrations were within the expected range with regard to the applied NO₂ concentrations,
22 RH and cover characteristics, one sample (orange in Fig. 8) showed a sharp short-term increase in the initial phase
23 followed by respective decrease, not in line with all other samples (compare Fig. 6). However, after 4 hours both VIS
24 irradiated samples showed virtually constant HONO emissions (-3.8 and $+1.6 \text{ ppt h}^{-1}$, respectively). The sample
25 illuminated with UV/VIS light (3 UV and 4 VIS lamps) showed a sustained sharp increase in the first 4 hours,
26 followed by persistent and very stable (decay rate as low as -0.5 ppt h^{-1}) HONO emissions at an about 3-fold higher
27 level compared to samples irradiated with VIS only.

28 Integrating the 20 hour experiments, 9.23×10^{15} (4.6 ppb*h, VISa), 1.53×10^{16} (7.7 ppb*h, VISb) and 4.01×10^{16} (20
29 ppb*h, UV/VIS) molecules of HONO were produced. This means between 7.7×10^{13} and 3.3×10^{14} molecules of
30 HONO per cm² of BSA geometric surface were formed. With respect to the different experimental conditions
31 concerning cover thickness, RH, and NO₂ concentrations, this is in a similar order of magnitude as found for humic
32 acid (2×10^{15} molecules cm⁻² in 13 hours) by Stemmler et al. (2006).

33 If BSA acts like a catalytic converter as in a Langmuir-Hinshelwood reaction each BSA molecule can react several
34 times with NO₂ to heterogeneously form HONO. As described in 3.1, BSA nitration is in competition with NO₂
35 surface reactions and only a limited number of NO₂ molecules could react with BSA forming HONO via nitration of
36 proteins and subsequent decomposition of nitrated proteins. A BSA molecule contains 21 tyrosine residues, which
37 could react with NO₂. But even a strong nitration agent such as TNM is not capable of nitrating all tyrosine residues



1 and a mean nitration degree of 19% was found (Peterson et al., 2001; Yang et al., 2010), i.e., 4 tyrosine residues of
 2 one BSA molecule can be nitrated to form HONO. As 2 mg of BSA was applied for each flow tube coating, a total of
 3 1.8×10^{16} protein molecules can be inferred. In 20 hours of irradiating with VIS light 13-22% of the accessible Tyr
 4 residues (4 each BSA molecule) would have been reacted. Irradiating with additional UV lights at least 56% of the
 5 tyrosine residues would have been nitrated and decomposed, respectively. But as NO_2 is a much weaker nitrating
 6 agent and nitration of only one tyrosine residue is probable (ND of BSA with O_3/NO_2 6%; Yang et al., 2010) up to
 7 85% BSA molecules would have been reacted when irradiated with VIS lights, and even more HONO molecules as
 8 coated BSA molecules would have been generated under UV/VIS light conditions. Other amino-acids of the protein
 9 like tryptophan or phenylalanine might also be nitrated but without formation of HONO (Goeschen et al., 2011).
 10 Hence, a contribution of heterogeneous conversion of NO_2 can be anticipated.

11 3.3 Kinetic studies

12 The experimental results (especially the stability over a long time) indicate that the formation of HONO from NO_2
 13 on protein surfaces likely underlies the Langmuir-Hinshelwood mechanism in which the protein would act as a
 14 catalytic converter (Fig. 9). The first step is the fast reversible physical adsorption of NO_2 (k_1) and water followed by
 15 the slow conversion into HONO (eq.1 and eq.2). In our experiments and in the atmosphere there is always sufficient
 16 water and for simplification we assume that the reaction rate only depends on NO_2 .

$$17 \quad \frac{d[\text{NO}_2]_s}{dt} = k_1 * [\text{NO}_2]_g \quad (\text{eq.1})$$

$$18 \quad \frac{d[\text{HONO}]_s}{dt} = k_2 * [\text{NO}_2]_s \quad (\text{eq.2})$$

19 where index s and g indicate sorbed and gaseous state, respectively.

20 From the experiments in which higher HONO concentrations were detected with higher light intensities we conclude
 21 that the heterogeneous conversion of NO_2 to HONO is light induced or a photochemical reaction. It was observed
 22 that the nitration of proteins is a competitive (side) reaction of the direct HONO formation (eq.2) but light induced
 23 decomposition of nitrated protein also produces HONO (eq.3).

$$24 \quad \frac{d[\text{HONO}]_s}{dt} = k_4 * k_5 * [\text{NO}_2]_s \quad (\text{eq.3})$$

25 As these two processes cannot be discriminated by the observations presented here, we combine both reactions to
 26 formulate an overall formation equation (eq.4) with $k' = k_2 + k_4 * k_5$

$$27 \quad \frac{d[\text{HONO}]_s}{dt} = [\text{HONO}]_s^1 + [\text{HONO}]_s^2 = k' * [\text{NO}_2]_s \quad (\text{eq.4})$$

28 The final step of the mechanism is the release of the generated HONO into the air. Since proteins are in general
 29 slightly acidic, the desorption of HONO (k_3) should be fairly fast (eq.5).

$$30 \quad \frac{d[\text{HONO}]_g}{dt} = k_3 * [\text{HONO}]_s \quad (\text{eq.5})$$

31 An effective formation rate of gaseous NO_2 to gaseous HONO k_{eff} was calculated according to eq.6.

$$32 \quad \frac{d[\text{HONO}]_g}{dt} = k_{\text{eff}} * [\text{NO}_2]_g \quad (\text{eq.6})$$

33 with $k_{\text{eff}} = k_1 * k' * k_3$

34 In the first 5-10 min of the long-term experiments HONO increased (Fig. 8 – zoomed in range). This slope was taken
 35 as $d[\text{HONO}]_g/dt$ in eq.6. Effective rate constants between $1.48 \times 10^{-6} \text{ s}^{-1}$ (VIS a) and $7.40 \times 10^{-6} \text{ s}^{-1}$ (VIS b) were



1 calculated. When irradiating with VIS light only, the concentration of HONO was either constant or decreased for 2
2 h after this first 10 min. When irradiating with additional UV light, the HONO signal showed an enhancement in two
3 steps. In the first 10 min it was strongly increasing (1327 ppt h^{-1}) and then in the next hour it increased less with 170
4 ppt h^{-1} prior to stabilization. Therefore two rate constants of $4.10 \times 10^{-6} \text{ s}^{-1}$ and $5.2 \times 10^{-7} \text{ s}^{-1}$ were obtained, respectively.
5 Reactive uptake coefficients for NO_2 were calculated according to Li et al. (2016). For both irradiation types the
6 uptake coefficient γ was in the range of 7×10^{-6} at the very beginning of each experiment. After a few minutes they
7 decreased to a mean of 1×10^{-7} . The calculated k_{eff} values and uptake coefficient are in the same range and match the
8 NO_2 uptake coefficients on irradiated humic acid surfaces (coatings) and aerosols obtained by Stemmler et al. (2006
9 and 2007) which were in between 2×10^{-6} and 2×10^{-5} (coatings) and 1×10^{-6} and 6×10^{-6} (aerosols), depending on NO_2
10 concentrations and light intensities. Similar NO_2 uptake coefficients on humic acid were observed by Han et al.
11 (2016). George et al., (2005) reported about a two-fold increased NO_2 uptake coefficients for irradiated organic
12 substrates (benzophenone, catechol, anthracene) compared to dark conditions, in the order of $(0.6-5) \times 10^{-6}$. NO_2
13 uptake coefficients on gentisic acid and tannic acid were in between $(3.3-4.8) \times 10^{-7}$ (Sosedova et al., 2011), still
14 being higher than on fresh soot or dust (about 1×10^{-7} ; Monge et al., 2010; Ndour et al., 2008). The NO_2 uptake
15 coefficients on BSA in presence of O_3 (1×10^{-5} , for 26 ppb NO_2 and 20 ppb O_3) published by Shiraiwa et al. (2012)
16 were somewhat higher than the values calculated here without O_3 but with light.
17 As proteins can efficiently be nitrated by O_3 and NO_2 in polluted air (Franze et al., 2005, Shiraiwa et al., 2012;
18 Reinmuth-Selzle et al. 2014), the emission of HONO from light-induced decomposing nitrated proteins could play an
19 important role in the HONO budget. As proteins are nitrated at their tyrosine residues (at the ortho position to the OH
20 group on the aromatic ring) the underlying mechanism of this HONO formation should be very similar to the HONO
21 formation by photolysis of ortho-nitrophenols described by Bejan et al. (2006). This starts with a photo-induced
22 hydrogen transfer from the OH group to the vicinal NO_2 group (Fig. 1), which leads to an excited intermediate from
23 which HONO is eliminated subsequently.

24 4. Summary and Conclusion

25 Photochemical nitration of proteins accompanied by formation of HONO by (i) heterogeneous conversion of NO_2
26 and (ii) by decomposition of nitrated proteins was studied under relevant atmospheric conditions. NO_2 concentrations
27 ranged from 20 ppb (typical for urban regions in Europe and USA) up to 100 ppb (representative for highly polluted
28 industrial regions). The applied relative humidity of up to 80% and light intensities of up to 161 W/m^2 are common
29 on cloudy days. Under illuminated conditions very low nitration of proteins or even no native protein was observed,
30 indicating a light-induced decomposition of nitrated proteins to shorter peptides. These might still include nitrated
31 residues of which potential health effects are not yet known. An average effective rate constant of the total NO_2 -
32 HONO conversion of $3.3 \times 10^{-6} \text{ s}^{-1}$ (for about 120 cm^2 of protein surface and a layer volume of 0.003 cm^3 ;
33 surface/volume ratio $\sim 40000 \text{ cm}^{-1}$) was obtained. At 20 ppb NO_2 238 ppt h^{-1} HONO would be formed. Projecting
34 this to 1 m^2 of pure BSA surface a formation of $19.8 \text{ ppb HONO h}^{-1} \text{ m}^{-2}$ could be estimated. No data about
35 representative protein surface areas on atmospheric aerosol particles are available. However, the number and mass
36 concentration of primary biological aerosol particles such as pollen, fungal spores and bacteria, containing proteins,



1 are in the range of $10\text{-}10^4\text{ m}^{-3}$ and $10^{-3}\text{-}1\text{ }\mu\text{g m}^{-3}$, respectively (Shiraiwa et al., 2012). Therefore it is difficult to
2 estimate the importance of HONO formation on protein surface and its contribution to the HONO budget. In many
3 studies the calculated un-known source strength of daytime HONO formation is with a range of about 200-800 ppt
4 h^{-1} (Kleffmann et al., 2005; Acker et al., 2006; Li et al., 2012).

5 **Acknowledgment**

6 This study was supported by the Max Planck Society (MPG).

7 **References**

- 8 Acker, K., Moller, D., Wieprecht, W., Meixner, F. X., Bohn, B., Gilge, S., Plass-Dulmer, C., and Berresheim, H.:
9 Strong daytime production of OH from HNO₂ at a rural mountain site, *Geophysical Research Letters*, 33, 2006.
10 Alfassi, Z. B.: Selective Oxidation of Tyrosine Oxidation by NO₂ and ClO₂ at basic pH, *Radiation Physics and*
11 *Chemistry*, 29, 405-406, 1987.
12 Aliche, B., Platt, U., and Stutz, J.: Impact of nitrous acid photolysis on the total hydroxyl radical budget during the
13 Limitation of Oxidant Production/Pianura Padana Produzione di Ozono study in Milan, *Journal of Geophysical*
14 *Research-Atmospheres*, 107, 2002.
15 Ammann, M., Kalberer, M., Jost, D. T., Tobler, L., Rossler, E., Pigué, D., Gaggeler, H. W., and Baltensperger, U.:
16 Heterogeneous production of nitrous acid on soot in polluted air masses, *Nature*, 395, 157-160, 1998.
17 Arens, F., Gutzwiller, L., Baltensperger, U., Gaggeler, H. W., and Ammann, M.: Heterogeneous reaction of NO₂ on
18 diesel soot particles, *Environmental Science & Technology*, 35, 2191-2199, 10.1021/es000207s, 2001.
19 Aubin, D. G., and Abbatt, J. P. D.: Interaction of NO₂ with hydrocarbon soot: Focus on HONO yield, surface
20 modification, and mechanism, *Journal of Physical Chemistry A*, 111, 6263-6273, 2007.
21 Bensasson RV, Land EJ, Truscott TG. Excited states and free radicals in biology and medicine. Oxford: Oxford
22 University Press; 1993.
23 Bejan, I., Abd El Aal, Y., Barnes, I., Benter, T., Bohn, B., Wiesen, P., and Kleffmann, J.: The photolysis of ortho-
24 nitrophenols: a new gas phase source of HONO, *Physical Chemistry Chemical Physics*, 8, 2028-2035, 2006.
25 Bujacz, A.: Structures of bovine, equine and leporine serum albumin, *Acta Crystallographica Section D*, 68, 1278-
26 1289, doi:10.1107/S0907444912027047, 2012.
27 Costabile, F., Amoroso, A., and Wang, F.: Sub-mu m particle size distributions in a suburban Mediterranean area.
28 Aerosol populations and their possible relationship with HONO mixing ratios, *Atmospheric Environment*, 44,
29 5258-5268, 2010.
30 D'Amato, G., Cecchi, L., Bonini, S., Nunes, C., Annesi-Maesano, I., Behrendt, H., Liccardi, G., Popov, T., and Van
31 Cauwenberge, P.: Allergenic pollen and pollen allergy in Europe, *Allergy*, 62, 976-990, 10.1111/j.1398-
32 9995.2007.01393.x, 2007.



- 1 Elshorbany, Y. F., Steil, B., Brühl, C., and Lelieveld, J.: Impact of HONO on global atmospheric chemistry
2 calculated with an empirical parameterization in the EMAC model, *Atmos. Chem. Phys.*, 12, 9977-10000,
3 doi:10.5194/acp-12-9977-2012, 2012.
- 4 Elshorbany, Y.F., P. Crutzen, B. Steil, A. Pozzer, and J. Lelieveld, Global and regional impacts of HONO on the
5 chemical composition of clouds and aerosols, *Atmos. Chem. Phys.*, 14, 1167-1184, 2014.
- 6 Finlayson-Pitts, B. J., Wingen, L. M., Sumner, A. L., Syomin, D., and Ramazan, K. A.: The heterogeneous
7 hydrolysis of NO₂ in laboratory systems and in outdoor and indoor atmospheres: An integrated mechanism,
8 *Physical Chemistry Chemical Physics*, 5, 223-242, 10.1039/b208564j, 2003.
- 9 Franze, T., Krause, K., Niessner, R., and Poeschl, U.: Proteins and amino acids in air particulate matter, *Journal of*
10 *Aerosol Science*, 34, S777-S778, 2003.
- 11 Franze, T., Weller, M. G., Niessner, R., and Pöschl, U.: Protein nitration by polluted air, *Environmental Science &*
12 *Technology*, 39, 2005.
- 13 George, C., Streckowski, R. S., Kleffmann, J., Stemmler, K., and Ammann, M.: Photoenhanced uptake of gaseous
14 NO₂ on solid-organic compounds: a photochemical source of HONO?, *Faraday Discussions*, 130, 195-210,
15 2005.
- 16 Goeschen, C., Wibowo, N., White, J. M., and Wille, U.: Damage of aromatic amino acids by the atmospheric free
17 radical oxidant NO₃[radical dot] in the presence of NO₂[radical dot], N₂O₄, O₃ and O₂, *Organic &*
18 *Biomolecular Chemistry*, 9, 3380-3385, 10.1039/C0OB01186J, 2011.
- 19 Gruijthuisen, Y. K., Grieshuber, I., Stoecklinger, A., Tischler, U., Fehrenbach, T., Weller, M. G., Vogel, L., Vieths,
20 S., Poeschl, U., and Duschl, A.: Nitration enhances the allergenic potential of proteins, *International Archives*
21 *of Allergy and Immunology*, 141, 265-275, 2006.
- 22 Han, C., Yang, W. J., Wu, Q. Q., Yang, H., and Xue, X. X.: Heterogeneous Photochemical Conversion of NO₂ to
23 HONO on the Humic Acid Surface under Simulated Sunlight, *Environmental Science & Technology*, 50, 5017-
24 5023, 2016.
- 25 Heland, J., Kleffmann, J., Kurtenbach, R., and Wiesen, P.: A new instrument to measure gaseous nitrous acid
26 (HONO) in the atmosphere, *Environmental Science & Technology*, 35, 3207-3212, 2001.
- 27 Houee-Levin, C., Bobrowski, K., Horakova, L., Karademir, B., Schoneich, C., Davies, M. J., and Spickett, C. M.:
28 Exploring oxidative modifications of tyrosine: An update on mechanisms of formation, advances in analysis
29 and biological consequences, *Free Radical Research*, 49, 347-373, 10.3109/10715762.2015.1007968, 2015.
- 30 Kalberer, M., Ammann, M., Arens, F., Gaggeler, H. W., and Baltensperger, U.: Heterogeneous formation of nitrous
31 acid (HONO) on soot aerosol particles, *Journal of Geophysical Research-Atmospheres*, 104, 13825-13832,
32 1999.
- 33 Kampf, C. J., Liu, F., Reinmuth-Selzle, K., Berkemeier, T., Meusel, H., Shiraiwa, M., and Pöschl, U.: Protein Cross-
34 Linking and Oligomerization through Dityrosine Formation upon Exposure to Ozone, *Environmental Science*
35 *& Technology*, 49, 10859-10866, 10.1021/acs.est.5b02902, 2015.
- 36 Kleffmann, J., H. Becker, K., Lackhoff, M., and Wiesen, P.: Heterogeneous conversion of NO₂ on carbonaceous
37 surfaces, *Physical Chemistry Chemical Physics*, 1, 5443-5450, 1999.



- 1 Kleffmann, J., Kurtenbach, R., Lorzer, J., Wiesen, P., Kalthoff, N., Vogel, B., and Vogel, H.: Measured and
2 simulated vertical profiles of nitrous acid - Part I: Field measurements, *Atmospheric Environment*, 37, 2949-
3 2955, 2003.
- 4 Kleffmann, J., Gavrioloaiei, T., Hofzumahaus, A., Holland, F., Koppmann, R., Rupp, L., Schlosser, E., Siese, M., and
5 Wahner, A.: Daytime formation of nitrous acid: A major source of OH radicals in a forest, *Geophysical*
6 *Research Letters*, 32, 2005.
- 7 Kurtenbach, R., Becker, K. H., Gomes, J. A. G., Kleffmann, J., Lorzer, J. C., Spittler, M., Wiesen, P., Ackermann,
8 R., Geyer, A., and Platt, U.: Investigations of emissions and heterogeneous formation of HONO in a road traffic
9 tunnel, *Atmospheric Environment*, 35, 3385-3394, 2001.
- 10 Lang-Yona, N., Shuster-Meiseles, T., Mazar, Y., Yarden, O., and Rudich, Y.: Impact of urban air pollution on the
11 allergenicity of *Aspergillus fumigatus* conidia: Outdoor exposure study supported by laboratory experiments,
12 *Science of The Total Environment*, 541, 365-371, <http://dx.doi.org/10.1016/j.scitotenv.2015.09.058>, 2016.
- 13 Levy, H.: Normal Atmosphere: Large Radical and Formaldehyde Concentrations Predicted, *Science*, 173, 141-143,
14 1971.
- 15 Li, X., Brauers, T., Haeseler, R., Bohn, B., Fuchs, H., Hofzumahaus, A., Holland, F., Lou, S., Lu, K. D., Rohrer, F.,
16 Hu, M., Zeng, L. M., Zhang, Y. H., Garland, R. M., Su, H., Nowak, A., Wiedensohler, A., Takegawa, N., Shao,
17 M., and Wahner, A.: Exploring the atmospheric chemistry of nitrous acid (HONO) at a rural site in Southern
18 China, *Atmospheric Chemistry and Physics*, 12, 1497-1513, 2012.
- 19 Li, G., Su, H., Li, X., Kuhn, U., Meusel, H., Hoffmann, T., Ammann, M., Pöschl, U., Shao, M., and Cheng, Y.:
20 Uptake of gaseous formaldehyde by soil surfaces: a combination of adsorption/desorption equilibrium and
21 chemical reactions, *Atmos. Chem. Phys.*, 16, 10299-10311, 10.5194/acp-16-10299-2016, 2016.
- 22 Menetrez, M. Y., Foarde, K. K., Dean, T. R., Betancourt, D. A., and Moore, S. A.: An evaluation of the protein mass
23 of particulate matter, *Atmospheric Environment*, 41, 8264-8274,
24 <http://dx.doi.org/10.1016/j.atmosenv.2007.06.021>, 2007.
- 25 Meusel, H., Kuhn, U., Reiffs, A., Mallik, C., Harder, H., Martinez, M., Schuladen, J., Bohn, B., Parchatka, U.,
26 Crowley, J. N., Fischer, H., Tomsche, L., Novelli, A., Hoffmann, T., Janssen, R. H. H., Hartogensis, O.,
27 Pikridas, M., Vrekoussis, M., Bourtsoukidis, E., Weber, B., Lelieveld, J., Williams, J., Pöschl, U., Cheng, Y.,
28 and Su, H.: Daytime formation of nitrous acid at a coastal remote site in Cyprus indicating a common ground
29 source of atmospheric HONO and NO, *Atmos. Chem. Phys.*, 16, 14475-14493, 10.5194/acp-16-14475-2016,
30 2016.
- 31 Miguel, A. G., Cass, G. R., Glovsky, M. M., and Weiss, J.: Allergens in paved road dust and airborne particles,
32 *Environmental Science & Technology*, 33, 4159-4168, 1999.
- 33 Mikhailov, E., Vlasenko, S., Niessner, R., and Pöschl, U.: Interaction of aerosol particles composed of protein and
34 salt with water vapor: hygroscopic growth and microstructural rearrangement, *Atmos. Chem. Phys.*, 4, 323-
35 350, 10.5194/acp-4-323-2004, 2004.
- 36 Monge, M. E., D'Anna, B., Mazri, L., Giroir-Fendler, A., Ammann, M., Donaldson, D. J., and George, C.: Light
37 changes the atmospheric reactivity of soot, *Proceedings of the National Academy of Sciences of the United*
38 *States of America*, 107, 6605-6609, 10.1073/pnas.0908341107, 2010.



- 1 Ndour, M., D'Anna, B., George, C., Ka, O., Balkanski, Y., Kleffmann, J., Stemmler, K., and Ammann, M.:
2 Photoenhanced uptake of NO₂ on mineral dust: Laboratory experiments and model simulations, *Geophysical*
3 *Research Letters*, 35, 10.1029/2007gl032006, 2008.
- 4 Neves-Petersen, M.T., Petersen, S., and Gajula, G.P. (2012): UV Light Effects on Proteins: From Photochemistry to
5 Nanomedicine, *Molecular Photochemistry - Various Aspects*, Dr. Satyen Saha (Ed.), InTech, DOI:
6 10.5772/37947. Available from: [http://www.intechopen.com/books/molecular-photochemistry-various-](http://www.intechopen.com/books/molecular-photochemistry-various-aspects/uv-light-effects-on-proteins-from-photochemistry-to-nanomedicine)
7 [aspects/uv-light-effects-on-proteins-from-photochemistry-to-nanomedicine](http://www.intechopen.com/books/molecular-photochemistry-various-aspects/uv-light-effects-on-proteins-from-photochemistry-to-nanomedicine).
- 8 Nikogosyan, D. N., and Gorner, H.: Laser-induced photodecomposition of amino acids and peptides: extrapolation to
9 corneal collagen, *IEEE Journal of Selected Topics in Quantum Electronics*, 5, 1107-1115,
10 10.1109/2944.796337, 1999.
- 11 Notholt, J., Hjorth, J., and Raes, F.: Formation of HNO₂ on aerosol surfaces during foggy periods in the presence of
12 NO and NO₂, *Atmospheric Environment Part a-General Topics*, 26, 211-217, 1992.
- 13 Oswald, R., Behrendt, T., Ermel, M., Wu, D., Su, H., Cheng, Y., Breuninger, C., Moravek, A., Mouglin, E., Delon,
14 C., Loubet, B., Pommerening-Roeser, A., Soergel, M., Poeschl, U., Hoffmann, T., Andreae, M. O., Meixner, F.
15 X., and Trebs, I.: HONO Emissions from Soil Bacteria as a Major Source of Atmospheric Reactive Nitrogen,
16 *Science*, 341, 1233-1235, 2013.
- 17 Petersson, A.-S., Steen, H., Kalume, D. E., Caidahl, K., and Roepstorff, P.: Investigation of tyrosine nitration in
18 proteins by mass spectrometry, *Journal of Mass Spectrometry*, 36, 616-625, 10.1002/jms.161, 2001.
- 19 Prutz, W. A.: Tyrosine Oxidation by NO₂ in aqueous-solution, *Zeitschrift Fur Naturforschung C-a Journal of*
20 *Biosciences*, 39, 725-727, 1984.
- 21 Prutz, W. A., Monig, H., Butler, J., and Land, E. J.: Reactions of nitrogen dioxide in aqueous model systems –
22 oxidation of tyrosine units in peptides and proteins, *Archives of Biochemistry and Biophysics*, 243, 125-134,
23 10.1016/0003-9861(85)90780-5, 1985.
- 24 Pummer, B. G., Budke, C., Augustin-Bauditz, S., Niedermeier, D., Felgitsch, L., Kampf, C. J., Huber, R. G., Liedl,
25 K. R., Loerting, T., Moschen, T., Schauerperl, M., Tollinger, M., Morris, C. E., Wex, H., Grothe, H., Pöschl, U.,
26 Koop, T., and Fröhlich-Nowoisky, J.: Ice nucleation by water-soluble macromolecules, *Atmos. Chem. Phys.*,
27 15, 4077-4091, 10.5194/acp-15-4077-2015, 2015.
- 28 Ramazan, K. A., Syomin, D., and Finlayson-Pitts, B. J.: The photochemical production of HONO during the
29 heterogeneous hydrolysis of NO₂, *Physical Chemistry Chemical Physics*, 6, 3836-3843, 2004.
- 30 Reinmuth-Selzle, K., Ackaert, C., Kampf, C. J., Samonig, M., Shiraiwa, M., Kofler, S., Yang, H., Gadermaier, G.,
31 Brandstetter, H., Huber, C. G., Duschl, A., Oostingh, G. J., and Pöschl, U.: Nitration of the Birch Pollen
32 Allergen Bet v 1.0101: Efficiency and Site-Selectivity of Liquid and Gaseous Nitrating Agents, *Journal of*
33 *Proteome Research*, 13, 1570-1577, 2014.
- 34 Reisinger, A. R.: Observations of HNO₂ in the polluted winter atmosphere: possible heterogeneous production on
35 aerosols, *Atmospheric Environment*, 34, 3865-3874, 2000.
- 36 Ren, X., Brune, W. H., Oliger, A., Metcalf, A. R., Simpas, J. B., Shirley, T., Schwab, J. J., Bai, C., Roychowdhury,
37 U., Li, Y., Cai, C., Demerjian, K. L., He, Y., Zhou, X., Gao, H., and Hou, J.: OH, HO₂, and OH reactivity



- 1 during the PMTACS-NY Whiteface Mountain 2002 campaign: Observations and model comparison, *Journal of*
2 *Geophysical Research-Atmospheres*, 111, 2006.
- 3 Riediker, Koller, and Monn: Differences in size selective aerosol sampling for pollen allergen detection using high-
4 volume cascade impactors, *Clinical & Experimental Allergy*, 30, 867-873, 10.1046/j.1365-2222.2000.00792.x,
5 2000.
- 6 Ring, J., Kramer, U., Schafer, T., and Behrendt, H.: Why are allergies increasing?, *Current Opinion in Immunology*,
7 13, 701-708, 2001.
- 8 Salgado, M. S., and Rossi, M. J.: Flame soot generated under controlled combustion conditions: Heterogeneous
9 reaction of NO₂ on hexane soot, *International Journal of Chemical Kinetics*, 34, 620-631, 10.1002/kin.10091,
10 2002.
- 11 Selzle, K.; Ackaert, C.; Kampf, C. J., et al., Determination of nitration degrees for the birch pollen allergen Bet v 1.
12 *Analytical and Bioanalytical Chemistry* 2013, 405 (27), 8945-8949.
- 13 Shiraiwa, M., Ammann, M., Koop, T., and Pöschl, U.: Gas uptake and chemical aging of semisolid organic aerosol
14 particles, *Proceedings of the National Academy of Sciences*, 108, 11003-11008, 10.1073/pnas.1103045108,
15 2011. Shiraiwa, M., Selzle, K., Yang, H., Sosedova, Y., Ammann, M., and Poeschl, U.: Multiphase Chemical
16 Kinetics of the Nitration of Aerosolized Protein by Ozone and Nitrogen Dioxide, *Environmental Science &*
17 *Technology*, 46, 6672-6680, 2012.
- 18 Sörgel, M., Regelin, E., Bozem, H., Diesch, J. M., Drewnick, F., Fischer, H., Harder, H., Held, A., Hosaynali-Beygi,
19 Z., Martinez, M., and Zetzsch, C.: Quantification of the unknown HONO daytime source and its relation to
20 NO₂, *Atmospheric Chemistry and Physics*, 11, 10433-10447, 2011.
- 21 Sörgel, M., Trebs, I., Wu, D., and Held, A.: A comparison of measured HONO uptake and release with calculated
22 source strengths in a heterogeneous forest environment, *Atmos. Chem. Phys.*, 15, 9237-9251, 10.5194/acp-15-
23 9237-2015, 2015.
- 24 Sosedova, Y., Rouviere, A., Bartels-Rausch, T., and Ammann, M.: UVA/Vis-induced nitrous acid formation on
25 polyphenolic films exposed to gaseous NO₂, *Photochemical & Photobiological Sciences*, 10, 1680-1690, 2011.
- 26 Stadler, D., and Rossi, M. J.: The reactivity of NO₂ and HONO on flame soot at ambient temperature: The influence
27 of combustion conditions, *Physical Chemistry Chemical Physics*, 2, 5420-5429, 10.1039/b005680o, 2000.
- 28 Staton, S. J. R., Woodward, A., Castillo, J. A., Swing, K., and Hayes, M. A.: Ground level environmental protein
29 concentrations in various ecuadorian environments: Potential uses of aerosolized protein for ecological
30 research, *Ecological Indicators*, 48, 389-395, <http://dx.doi.org/10.1016/j.ecolind.2014.08.036>, 2015.
- 31 Stemmler, K., Ammann, M., Donders, C., Kleffmann, J., and George, C.: Photosensitized reduction of nitrogen
32 dioxide on humic acid as a source of nitrous acid, *Nature*, 440, 195-198, 2006.
- 33 Stemmler, K., Ndour, M., Elshorbany, Y., Kleffmann, J., D'Anna, B., George, C., Bohn, B., and Ammann, M.: Light
34 induced conversion of nitrogen dioxide into nitrous acid on submicron humic acid aerosol, *Atmospheric*
35 *Chemistry and Physics*, 7, 4237-4248, 2007.
- 36 Su, H., Cheng, Y. F., Shao, M., Gao, D. F., Yu, Z. Y., Zeng, L. M., Slanina, J., Zhang, Y. H., and Wiedensohler, A.:
37 Nitrous acid (HONO) and its daytime sources at a rural site during the 2004 PRIDE-PRD experiment in China,
38 *Journal of Geophysical Research-Atmospheres*, 113, 2008b.



- 1 Su, H., Cheng, Y., Oswald, R., Behrendt, T., Trebs, I., Meixner, F. X., Andreae, M. O., Cheng, P., Zhang, Y., and
2 Poeschl, U.: Soil Nitrite as a Source of Atmospheric HONO and OH Radicals, *Science*, 333, 1616-1618, 2011.
- 3 Sumner, A. L., Menke, E. J., Dubowski, Y., Newberg, J. T., Penner, R. M., Hemminger, J. C., Wingen, L. M.,
4 Brauers, T., and Finlayson-Pitts, B. J.: The nature of water on surfaces of laboratory systems and implications
5 for heterogeneous chemistry in the troposphere, *Physical Chemistry Chemical Physics*, 6, 604-613,
6 10.1039/B308125G, 2004.
- 7 Villena, G., Wiesen, P., Cantrell, C. A., Flocke, F., Fried, A., Hall, S. R., Hornbrook, R. S., Knapp, D., Kosciuch, E.,
8 Mauldin, R. L., McGrath, J. A., Montzka, D., Richter, D., Ullmann, K., Walega, J., Weibring, P., Weinheimer,
9 A., Staebler, R. M., Liao, J., Huey, L. G., and Kleffmann, J.: Nitrous acid (HONO) during polar spring in
10 Barrow, Alaska: A net source of OH radicals?, *Journal of Geophysical Research: Atmospheres*, 116, n/a-n/a,
11 2011.
- 12 Vogel, B., Vogel, H., Kleffmann, J., and Kurtenbach, R.: Measured and simulated vertical profiles of nitrous acid -
13 Part II. Model simulations and indications for a photolytic source, *Atmospheric Environment*, 37, 2957-2966,
14 2003.
- 15 Weber, B., Wu, D., Tamm, A., Ruckteschler, N., Rodriguez-Caballero, E., Steinkamp, J., Meusel, H., Elbert, W.,
16 Behrendt, T., Soergel, M., Cheng, Y., Crutzen, P. J., Su, H., and Poeschi, U.: Biological soil crusts accelerate
17 the nitrogen cycle through large NO and HONO emissions in drylands, *Proceedings of the National Academy
18 of Sciences of the United States of America*, 112, 15384-15389, 2015.
- 19 Wong, K. W., Tsai, C., Lefer, B., Haman, C., Grossberg, N., Brune, W. H., Ren, X., Luke, W., and Stutz, J.: Daytime
20 HONO vertical gradients during SHARP 2009 in Houston, TX, *Atmospheric Chemistry and Physics*, 12, 635-
21 652, 2012.
- 22 Yang, H.; Zhang, Y. Y.; Pöschl, U., Quantification of nitrotyrosine in nitrated proteins. *Analytical and Bioanalytical
23 Chemistry* 2010, 397 (2), 879-886.
- 24 Zhang, Y. Y.; Yang, H.; Pöschl, U., Analysis of nitrated proteins and tryptic peptides by HPLC-chip-MS/MS: site-
25 specific quantification, nitration degree, and reactivity of tyrosine residues. *Analytical and Bioanalytical
26 Chemistry* 2011, 399 (1), 459-471.
- 27 Zhang, Q., and Anastasio, C.: Free and combined amino compounds in atmospheric fine particles (PM_{2.5}) and fog
28 waters from Northern California, *Atmospheric Environment*, 37, 2247-2258, 2003.
- 29 Zhou, X. L., Beine, H. J., Honrath, R. E., Fuentes, J. D., Simpson, W., Shepson, P. B., and Bottenheim, J. W.:
30 Snowpack photochemical production of HONO: a major source of OH in the Arctic boundary layer in
31 springtime, *Geophysical Research Letters*, 28, 4087-4090, 2001.
- 32 Zhou, X. L., Civerolo, K., Dai, H. P., Huang, G., Schwab, J., and Demerjian, K.: Summertime nitrous acid chemistry
33 in the atmospheric boundary layer at a rural site in New York State, *Journal of Geophysical Research-
34 Atmospheres*, 107, 2002a.
- 35 Zhou, X. L., Gao, H. L., He, Y., Huang, G., Bertman, S. B., Civerolo, K., and Schwab, J.: Nitric acid photolysis on
36 surfaces in low-NO_x environments: Significant atmospheric implications, *Geophysical Research Letters*, 30,
37 2003.
- 38



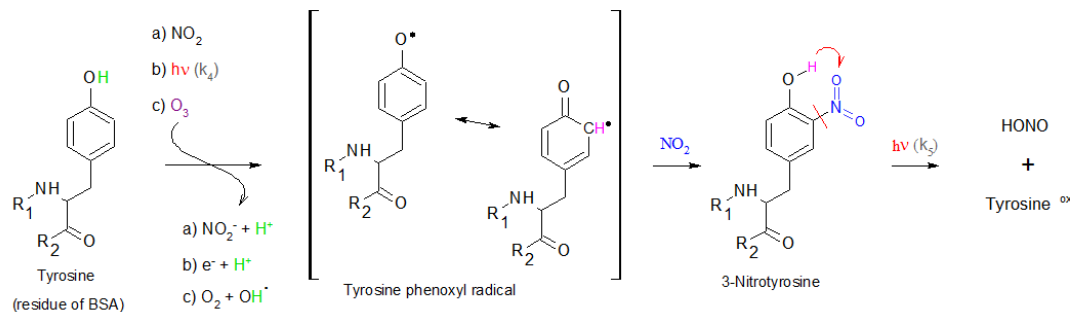
1 **Tables and Figures**

2 **Tab 1: Details on the different experiments, aims and experimental conditions (coating, applied NO₂ concentration,**
 3 **number of lights switched on, relative humidity and time for each exposure step):**

		Coating density (number of monolayers NML _f , thickness)	NO ₂ [ppb]	no. of lamps	RH [%]	time per step [h]
A light induced decomposition of nitrated protein and HONO formation						
1	light and NO ₂ dependency	n-OVA 21.5 ± 0.8 µg cm ⁻² (68 NML _f , 298.05 nm)	0-20	0-1-3-7 VIS	50	1
B heterogeneous NO₂ transformation on BSA						
2	NO ₂ dependency	BSA 16.1±0.4 µg cm ⁻² (50 NML _f , 217.6 nm)	0-20-40-60-100	7 VIS	50	0.5-1
3	light dependency	BSA 31.4±1.4 µg cm ⁻² (99 NML _f , 435.2 nm)	20	0-1-3-7 VIS	50	0.5-1
4	coating thickness	BSA 16.1±0.4 µg cm ⁻² (50 NML _f , 217.6 nm), 22.5±0.8 µg cm ⁻² (71 NML _f , 310.8 nm), 31.4±1.4 µg cm ⁻² (99 NML _f , 435.2 nm)	20	7 VIS		0.5-3
5	RH dependency	BSA 17.5±0.4 µg cm ⁻² (55 NML _f , 241.7 nm)	25	0-7VIS	0-50-80	0.25-1
6	time effect	BSA 17.5±0.4 µg cm ⁻²	100	7 VIS	75	20
7	time effect	BSA 17.5±0.4 µg cm ⁻²	100	4 VIS + 3 UV	75	20

4 NML_f numbers of monolayers in flat orientation

5
6
7
8
9

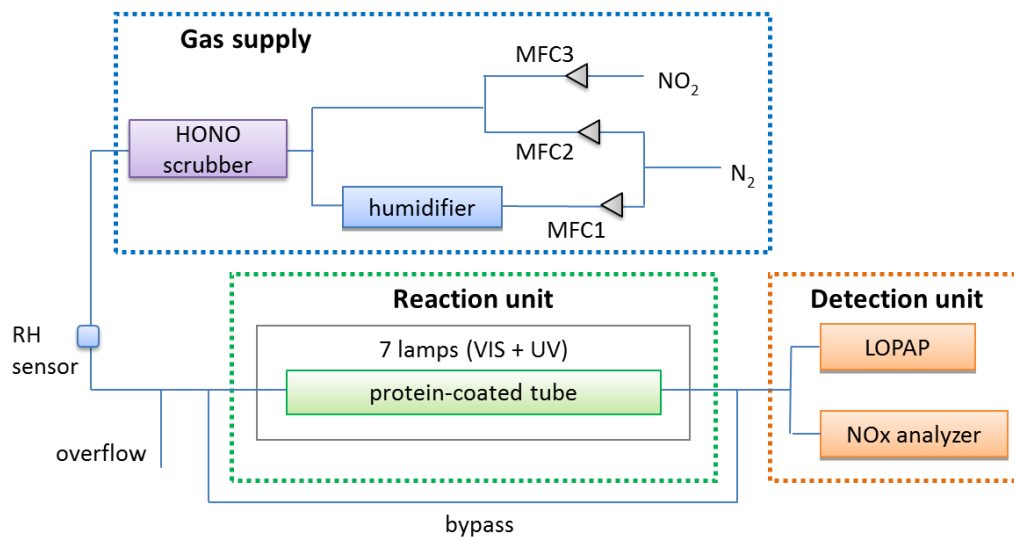


14 **Fig. 1: Reaction mechanism of atmospheric BSA nitration and subsequent HONO emission (formation of the tyrosine**
 15 **phenoxyl radical and following NO₂ addition to 3-nitrotyrosine was adapted from Houée-Levin et al. (2015) and Shiraiwa**
 16 **et al. (2012); intramolecular H-transfer adapted from Bejan et al., 2006).**

14
15
16
17



1



2

3 Fig. 2: flow system and set-up, MFC = mass flow controller

4

5

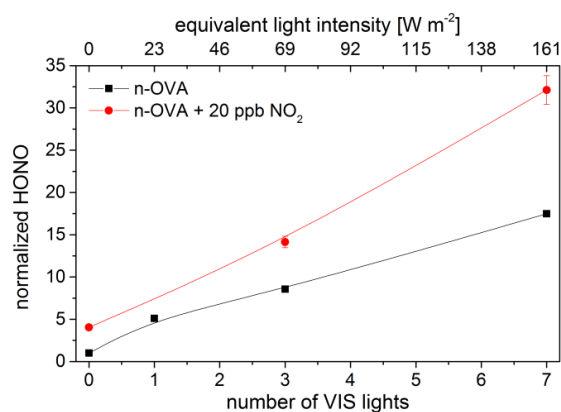
6

7

8

9

10



11

12 Fig. 3: Light enhanced HONO formation from proteins nitrated in the liquid phase prior to the flow tube experiments (n-
 13 OVA: ND 12.5%, coating 21.5 μg cm⁻²) with and without additional NO₂ in the purging air at 50% RH (HONO is
 14 normalized to the HONO concentration measured without NO₂ and no light ($[\text{HONO}]_{\text{lights; NO}_2} / [\text{HONO}]_{\text{dark; NO}_2=0}$).

15

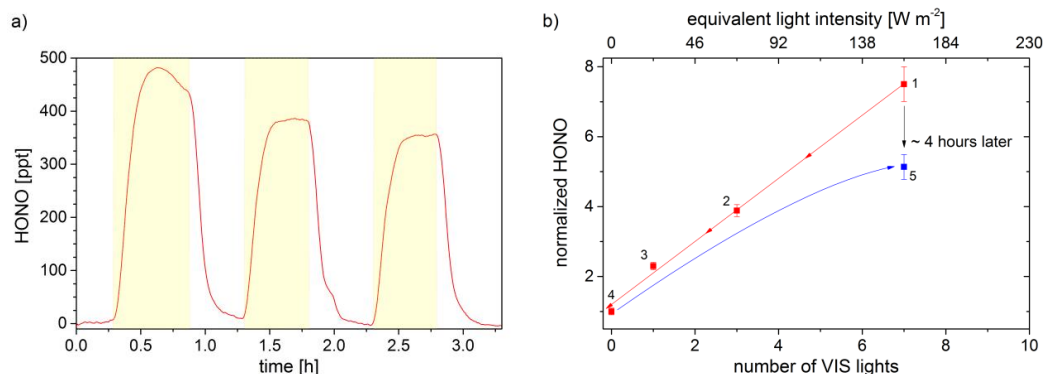
16

17

18



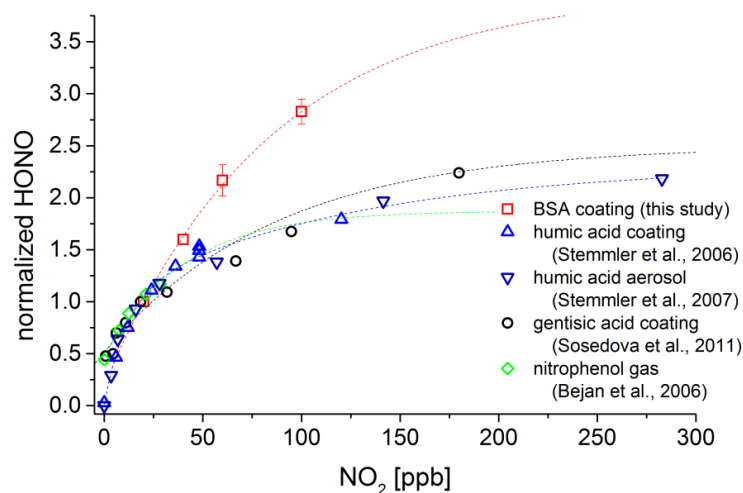
1



2

3 **Fig. 4:** a) Light enhancement of HONO formation on BSA surface ($22.5 \mu\text{g cm}^{-2}$), yellow shaded areas indicate periods in
 4 which 7 VIS lamps were switched on (RH = 50%, $\text{NO}_2 = 20 \text{ ppb}$); b) Dependency of HONO formation on radiation
 5 intensity at 20 ppb NO_2 and 50% RH (BSA = $31.4 \mu\text{g cm}^{-2}$). The experiment started with 7 VIS lights switched on,
 6 sequentially decreasing the number of lights (red symbols, nominated 1-4), prior to apply the initial irradiance again (blue
 7 symbol, 5). HONO was normalized to the HONO concentration in darkness ($[\text{HONO}]_{\text{lights}}/[\text{HONO}]_{\text{dark}}$). Error bars
 8 indicate standard deviation of 20-30 min measurements, standard deviation of point 5 covers 2.75 h measurement.

9

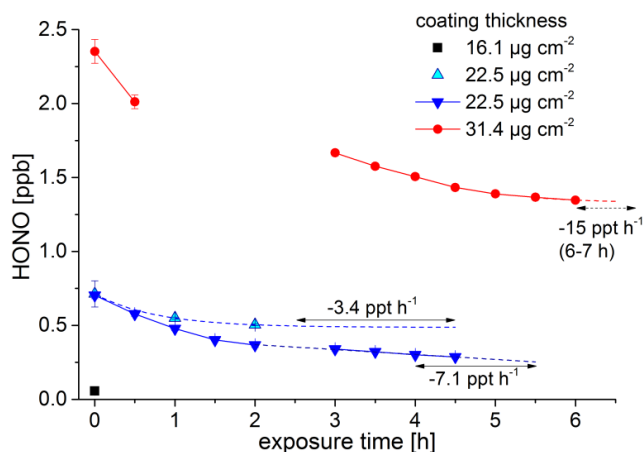


10

11 **Fig. 5:** Comparison of HONO formation dependency on NO_2 at different organic surfaces. HONO concentrations are
 12 normalized to the HONO concentration at 20 ppb NO_2 ($[\text{HONO}]_{\text{NO}_2}/[\text{HONO}]_{\text{NO}_2=20\text{ppb}}$). Red square = BSA coating ($16 \mu\text{g}$
 13 cm^{-2}) at 161 W m^{-2} and 50% RH (this study), blue triangles pointing up = humic acid coating ($8 \mu\text{g cm}^{-2}$) at 162 W m^{-2} and
 14 20% RH (Stemmler et al., 2006), dark blue triangles pointing down = humic acid aerosol with 100 nm diameter and a
 15 surface of $0.151 \text{ m}^2 \text{ m}^{-3}$ at 26% RH and $1 \times 10^{17} \text{ photons cm}^{-2} \text{ s}^{-1}$ (Stemmler et al., 2007), black circles = gentisic acid coating
 16 ($160\text{-}200 \mu\text{g cm}^{-2}$) at 40-45% RH and light intensity similar as in the humic acid aerosol case (Sosedova et al., 2011), green
 17 diamonds = ortho-nitrophenol in gas phase (ppm level) illuminated with UV/VIS light.

18

19

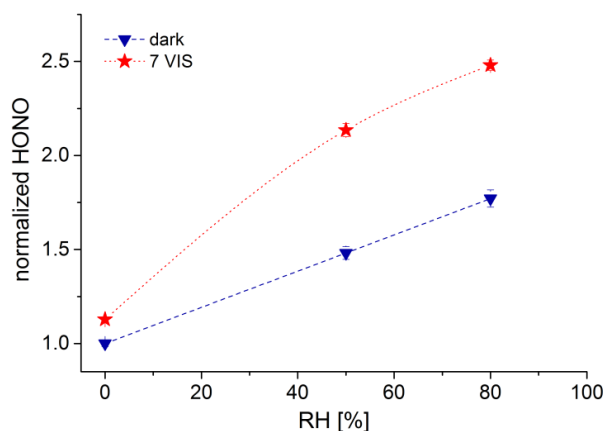


1

2 **Fig. 6: HONO formation on three different BSA coating thicknesses, exposed to 20 ppb of NO₂ under illuminated**
 3 **conditions (7 VIS lamps). The HONO concentrations were normalized to reaction tube coverage (black: 100% of reaction**
 4 **tube was covered with BSA, blueish: 70% of tube was covered and red: 50% of tube was covered with BSA). The middle**
 5 **thick coating (22.46 µg cm⁻²) was replicated and studied with different reaction times (cyan and blue triangle). Solid lines**
 6 **(with circles or triangles) present continuous measurements, when those are interrupted other conditions (e.g. light**
 7 **intensity, NO₂ concentration) prevailed. Dotted lines show interpolations. Arrows indicate the intervals in which the**
 8 **shown decay rates were determined. Error bars indicates standard deviations from 10-20 measuring points (5-10 min).**

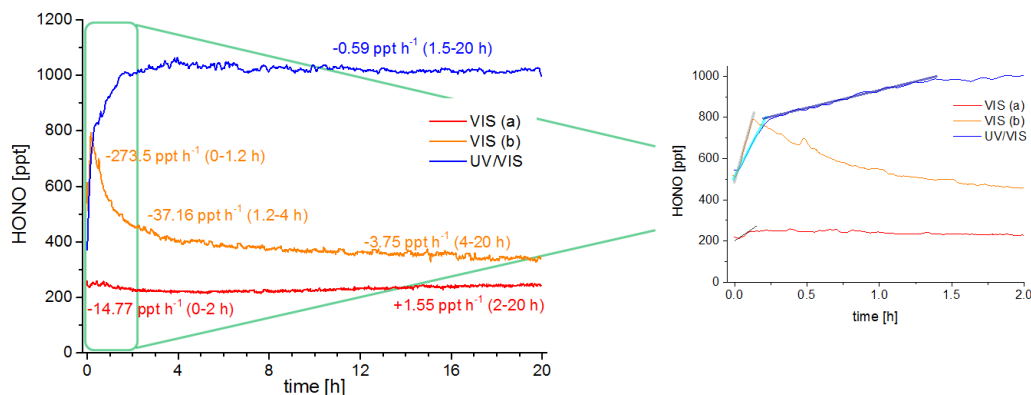
9

10



11

12 **Fig. 7: Dependency of humidity on the transformation of 25 ppb NO₂ in darkness (blue triangle) and with 7 VIS lights (red**
 13 **star). HONO was normalized to HONO concentrations in darkness under dry conditions**
 14 **($[\text{HONO}]_{\text{lights on-off}} / \text{RH} / [\text{HONO}]_{\text{dark}}; \text{RH}=0$).**

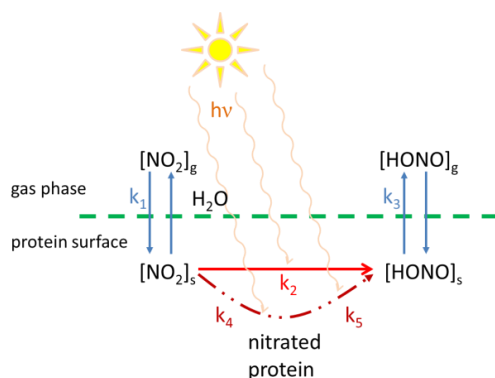


1

2 **Fig. 8:** Extended (20 h) measurements of light-enhanced HONO formation on BSA (three coatings of $17.5 \mu\text{g cm}^{-2}$) at 80%
 3 RH, 100 ppb NO_2 . HONO decay rates [ppt h^{-1}] are shown with time periods (in brackets) in which they were calculated,
 4 suggesting a stable HONO formation after 4 hours. Right: zoom in on the first 2 hours. Straight lines (black, grey, light
 5 and dark blue) show the regressions of which $d[\text{HONO}]/dt$ were used in the kinetic studies.

6

7



8

9 **Fig. 9:** Schematic illustration of the underlying Langmuir-Hinshelwood-mechanism of light induced HONO formation on
 10 protein surface.